pp 329-338, Adriatica Editrice, Bari, Italy.
Dilley, R. A., & Schreiber, U. (1984) *J. Bioenerg. Biomembr. 16*, 173-193.
Ferguson, S. J. (1985) *Biochim. Biophys. Acta 811*, 47-95.
Ferguson, S. J., & Sorgato, M. C. (1982) *Annu. Rev. Biochem. 51*, 185-217.
Giersch, C., & Meyer, M. (1984) *Biochem. Bioenerg. 12*, 63-71.
Karlish, J. D. S., & Avron, M. (1968) *Biochim. Biophys. Acta 153*, 878-888.
Karlish, S. J. D., & Avron, M. (1971) *Eur. J. Biochem. 20*, 51-57.
Laszlo, J. A., Baker, G. M., & Dilley, R. A. (1984) *J. Bioenerg. Biomembr. 16*, 37-51.
McCarty, R. E. (1982) *Ann. N.Y. Acad. Sci. 402*, 84-90.
McCarty, R. E., Fuhrman, J. S., & Tsuchiya, Y. (1971) *Proc. Natl. Acad. Sci. U.S.A. 68*, 2522-2526.
Mitchell, P. (1966) *Chemiosmotic Coupling in Oxidative and Photosynthetic Phosphorylation*, Glyn. Research Laboratories, Bodmin Cornwall, England.
Mitchell, P. (1979) *Science (Washington, D.C.) 206*, 1148-1159.
Nelson, N., Eytan, E., Notsani, B. E., Sigrist, H., Sigrist-Nelson, K., & Gitler, C. (1977) *Proc. Natl. Acad. Sci. U.S.A. 74*, 2375-2378.
Opanasenko, V. K., Ped'ko, T. P., Kuz'mina, V. P., & Yagushinsky, L. S. (1985) *FEBS Lett. 187*, 257-260.
Pick, U., & Avron, M. (1976) *Eur. J. Biochem. 70*, 569-576.
Prochaska, L. J., & Dilley, R. A. (1978a) *Arch. Biochem. Biophys. 187*, 61-71.
Prochaska, L. J., & Dilley, R. A. (1978b) *Biochem. Biophys. Res. Commun. 83*, 664-672.
Rottenberg, H. (1983) *Proc. Natl. Acad. Sci. U.S.A. 80*, 3313-3317.
Rottenberg, H. (1985) *Mod. Cell Biol. 4*, 47-83.
Rottenberg, H., & Hashimoto, K. (1986) *Biochemistry 25*, 1747-1755.
Rottenberg, H., & Steiner-Mordoch, S. (1986) *FEBS Lett. 202*, 314-318.
Schönfeld, M., & Neumann, J. (1977) *FEBS Lett. 73*, 51-54.
Schuldiner, S., Rottenberg, H., & Avron, M. (1972) *Eur. J. Biochem. 25*, 64-70.
Shahak, Y. (1982) *Plant Physiol. 70*, 87-91.
Theg, S. M., & Homann, P. H. (1982) *Biochim. Biophys. Acta 679*, 221-234.
Theg, S. M., & Junge, W. (1983) *Biochim. Biophys. Acta 723*, 294-307.
Westerhoff, H. V., Melandri, B. A., Venturoli, G., Azzone, G. F., & Kell, D. B. (1984) *Biochim. Biophys. Acta 768*, 253.
Williams, R. P. J. (1959) *Enzymes (2nd Ed.)*, 391-441.
Williams, R. P. J. (1961) *J. Theor. Biol. 1*, 1-13.
Williams, R. P. J. (1976) *Trends Biochem. Sci. (Pers. Ed.) 3*, N58-N61.

Characterization of Long-Range Electron Transfer in Mixed-Metal [Zinc,Iron] Hybrid Hemoglobins†

Jacqueline L. McGourty,‡ Sydney E. Peterson-Kennedy,§ Winnie Y. Ruo, and Brian M. Hoffman*
Department of Chemistry and Department of Biochemistry, Molecular Biology and Cell Biology, Northwestern University, Evanston, Illinois 60201

Received April 8, 1987; Revised Manuscript Received June 24, 1987

ABSTRACT: Measurements characterizing electron transfer from a photoexcited zinc protoporphyrin triplet (^{3}ZnP) to a ferriheme electron acceptor within the $[\alpha_1,\beta_2]$ electron-transfer complex of [Fe^{III},Zn] hybrid hemoglobins are reported. Analytical results demonstrate that the hybrids studied are pure, homogeneous proteins with 1:1 ZnP:FeP content. Within the T quaternary structure adopted by these hybrids, the optical spectrum of a Fe^{III}P is perturbed by the protein environment. Room temperature kinetic studies of the rate of ^{3}ZnP decay as a function of the heme oxidation and ligation state demonstrate that quenching of ^{3}ZnP by $Fe^{III}(H_2O)$P occurs by long-range intramolecular electron transfer with rate constant k_t = 100 (±10) s^{-1} and is not complicated by spin-quenching or energy-transfer processes; results are the same for α(Zn) and β(Zn) hybrids. Replacement of H_2O as a ligand to the ferriheme changes the ^{3}ZnP → Fe^{III}P electron-transfer rate constant, k_t, which demonstrates that electron transfer, not conformational conversion, is rate limiting. However, the trend is not readily explained by simple considerations of spin-state and bonding geometry: k_t decreases in the order imidazole > H_2O > F^- ~ CN^- ~ N_3^-. The reverse electron-transfer process $Fe^{II}P \rightarrow ZnP^+$ has not been observed directly but has been shown to be much more rapid, with rate constant $k_b > 10^3$ s^{-1}, consistent with the possible importance of "hole" superexchange in electron tunneling within protein complexes.

Long-range electron transfer can be studied without the complication of second-order processes by use of modified proteins that hold an electron donor/acceptor redox pair held at fixed distance (Marcus & Sutin, 1985; Mayo et al., 1986; Tollin et al., 1986). For example, Gray and co-workers (Winkler et al., 1982; Scott et al., 1985; Crutchley et al., 1985) and Isied and co-workers (Isied et al., 1982, 1984) have developed a technique for studying electron transfer *within* a protein. They show that $[(L)_5Ru]^{2+}$, bound to a histidine residue on the outside of a redox protein, such as ferricytochrome *c*, can exchange an electron with a redox center

† This research was supported by National Institutes of Health Grant HL-13531.
* Correspondence should be addressed to this author.
‡ Present address: Department of Chemistry, University of California, Davis, CA 95616.
§ Present address: Department of Chemistry, Whitworth College, Spokane, WA 99251.

0006-2960/87/0426-8302$01.50/0

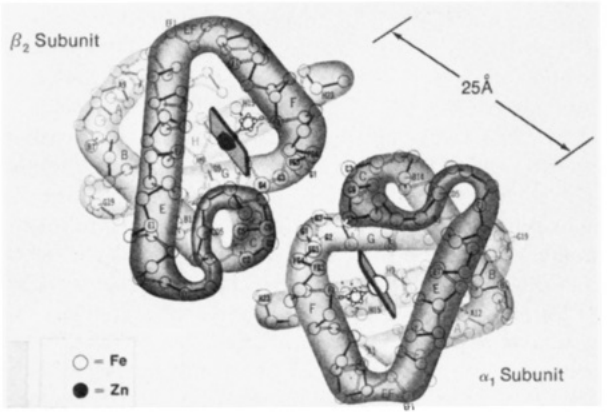

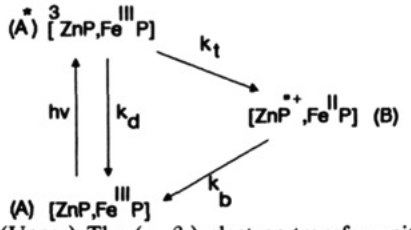

FIGURE 1: (Upper) The (α_1,β_2) electron-transfer unit. (Lower) Proposed kinetic scheme for electron transfer following flash excitation.

located on the inside of the protein. We (McGourty et al., 1983; Ho et al., 1984; Peterson-Kennedy et al., 1985), and subsequently McLendon and co-workers (Simolo et al., 1984; McLendon et al., 1985), have developed an alternate approach by which to study electron transfer *between* proteins. The heme in one protein of a tightly bound electron-transfer complex is replaced by a zinc protoporphyrin (ZnP).[1] Photoexcitation produces the ^{3}ZnP, which can transfer an electron to a ferriheme located in the protein partner. The charge-transfer intermediate thus formed returns to the ground state by back electron transfer from $Fe^{II}P$ to the cation radical ZnP^+ (Liang et al., 1986) (Figure 1).

Our initial report of such measurements employed [Zn,Fe] mixed-metal hemoglobin hybrids (McGourty et al., 1983), which provide an optimal system for detailed studies where the redox centers are held rigidly at fixed and crystallographically known distance and orientation. Hemoglobin is an [α_2,β_2] tetramer, and the [Zn,Fe] hybrid Hb can be prepared by substituting ZnP for the hemes of a single type of subunit, either α or β (Leonard et al., 1974; Blough, 1982). In the deoxyhemoglobin structure (Fermi & Perutz, 1981) normally adopted by these hybrids (Blough et al., 1980), the prosthetic groups of closest approach are α_1^{Fe}–β_2^{Zn}, Figure 1. The ZnP and FeP are roughly parallel, as in a hypothetical model for the electron-transfer complex between cytochrome *c* and cytochrome *c* peroxidase (Poulos & Finzel, 1984; Poulos & Kraut, 1980), and are separated by a heme pocket wall from each chain. The metal–metal distance is 25 Å, with shorter distances between atoms of the porphyrins. Since the α_1^{Fe}–β_1^{Zn} distances are much longer (Fe–Zn, 37 Å), for present purposes we may imagine the molecule as two independent electron-transfer complexes, each composed of an α_1–β_2 subunit pair.

[1] Abbreviations: IHP, inositol hexaphosphate; NEM, *N*-ethylmaleimide; PDS, dithiobis(pyridine); Hb, hemoglobin; metHb, ferric Hb; P, protoporphyrin IX; ZnP, zinc(II) protoporphyrin IX; ^{3}ZnP, excited zinc porphyrin triplet state; imid, imidazole; pyr, pyridine; *R*, $=A(424)/A(406)$; [Zn,Fe], hemoglobin derivative in which the two chains of a single type, α or β, are substituted with ZnP (When the specific oxidation and/or ligation state is of importance, it is indicated, e.g., [Zn,Fe^{II}CO]. When a particular hybrid is discussed, it is so indicated, e.g., [α-($Fe^{III}H_2O$),β(Zn)]).

For intramolecular ^{3}ZnP → $Fe^{III}(H_2O)$P, electron transfer within the α_1–β_2 complex of the [Zn,$Fe^{III}H_2O$] hybrid (Figure 1) occurs at a rate of $k_t \sim 100\ s^{-1}$ at room temperature. The process is strongly dependent on temperature, and we recently presented the first observation of low-temperature electron-nuclear tunneling within this crystallographically defined protein complex (Peterson-Kennedy et al., 1984, 1986).

Many elements of this ZnP strategy for studying protein complexes optimally presented in the Hb hybrids have not been described. We begin by discussing the characterization of the [Zn,Fe] hybrids. Next, we offer the first complete demonstration for a system utilizing the strategy of ZnP substitution, that the process being discussed is indeed intramolecular long-range electron transfer between the protein partners and that the measurements are not compromised by (i) intermolecular processes, (ii) paramagnetic quenching, or (iii) energy-transfer processes. The demonstrations heavily involve control experiments that vary the ligation state of the ferro- and ferrihemes of Hb and are not possible with complexes, such as those involving cytochrome *c* (Liang et al., 1986; Ho et al., 1985) or b_5 (Simolo et al., 1984) in which the heme-containing partner utilizes only endogenous axial ligands; here, electron transfer is best proven by observation of the reverse, $Fe^{II}P \rightarrow ZnP^+$, process (Liang et al., 1986). Therefore, the present work is of particular importance as a reference point for studies that utilize the ZnP approach.

We also describe some effects on electron transfer of ligand binding to the ferriheme electron acceptor. We find that the replacement of H_2O as a ligand to the ferriheme can increase *or* decrease the ^{3}ZnP → Fe^{III}P transfer rate, which is confirmatory that electron transfer and not conformational interconversion is rate limiting (Hoffman & Ratner, 1987). However, the trends are not readily explained by simple considerations of spin-state and bonding geometry. The reverse electron-transfer process, $Fe^{II}P \rightarrow ZnP^+$, has not been observed directly but has been shown to be much more rapid, with rate constant $k_b > 10^3\ s^{-1}$, consistent with the possible importance of "hole" superexchange in electron tunneling within protein complexes.

Materials and Methods

Materials

Blood was obtained from a local hospital. Precast, analytical ampholine PAG plates (pH 5.5–8.5) and Immobilines (pH 6.8–7.8) for preparative-scale PAG for isoelectric focusing were purchased from LKB. ZnP was prepared from the protoporphyrin disodium salt (Aldrich) and zinc acetate by the method of Adler et al. (1970). All purchased chemicals were used without further purification.

[Zn,Fe] hybrid hemoglobins were prepared by the method of Blough (Blough, 1981; Blough et al., 1982). Pooled red cells were washed and lysed, and hemoglobin (Hb) was purified by cation-exchange chromatography on CM-cellulose. α and β chains were then isolated from the tetramer by reaction with *p*-mercuribenzoate (Aldrich) followed by separation of the chains by the two-column procedure of Geraci et al. (1969). Chain globin was prepared by a method similar to that described by Yip et al. (1977) with slight modification (Blough, 1982). This globin was recombined with the opposite native chain to form a semiglobin that was subsequently reconstituted with ZnP. Final purification of the [Zn,Fe] hybrids was achieved by anion-exchange chromatography on DEAE-cellulose (Whatman) with a linear pH and salt gradient to separate reaction intermediates. Fully substituted zinc hemoglobin (ZnHb) was prepared, as described (Scholler et al.,

1978). All Fe-containing proteins were stored under CO in the $Fe^{II}(CO)P$ form. Zinc-substituted hemoproteins are light sensitive in the air. Therefore, all manipulations were performed anaerobically and/or in the dark.

Aquomethemoglobin (metHb) was prepared by addition of a 1.1–1.2-fold excess per Fe heme of $K_3Fe(CN)_6$ (Allied Chemical) to a stock protein solution. The reaction was monitored spectrophotometrically to completion (~30 min). Excess oxidant was removed by size-exclusion column chromatography with G-25 Sephadex (Sigma). This same procedure was used for oxidation of hybrids and reoxidation of photoreduced samples.

The reduced, unliganded forms of the hybrid, $[Zn,Fe^{II}]$, and of Hb were prepared by three separate methods, each of which yielded the same result. Flushing of the concentrated stock solution of $[Zn,Fe^{II}(CO)]$ hybrid with prepurified N_2 (Matheson) was sufficient to remove CO from the ferrous subunits. Alternatively, the aquomet species was reduced by addition of a stoichiometric amount of sodium dithionite. Occasionally, the deoxy species was prepared by reaction of the cyanomet species with sodium dithionite.

Unless noted, solutions were ~3 μM in Hb tetramer and ~10 μM in inositol hexaphosphate (IHP) and were prepared in 0.01 M KP_i buffer, pH 7.0 (KH_2PO_4 and $K_2HPO_4 \cdot 3H_2O$ from Mallinckrodt). Samples for kinetic measurements were in all cases made rigorously air free with the use of prepurified nitrogen (Matheson) and a Schlenk line. Anaerobic hybrid or Hb samples were prepared by first deaerating a small aliquot of the protein stock solution by gently flushing with N_2. This solution was then added to a previously degassed tonometer containing buffer solution that had been degassed for 30 min by purging with prepurified N_2.

Samples to be studied in the presence of CO were prepared by flushing a previously deoxygenated sample with ~99.5% CO (~0.5% N_2) (Matheson) for 15–20 min subsequent to sample preparation; a very gentle flow was used, to avoid denaturation of the protein via evaporation of the solvent. Flash photolysis of such samples could be used to monitor either the formation of ^{3}ZnP (Zemel & Hoffman, 1981; Peterson-Kennedy et al., 1986) or the expulsion of CO from the $Fe^{II}(CO)P$ (Blough et al., 1980; Blough, 1982).

Search for a possible concentration dependence utilized samples that were between 5 and 35 μM in heme. Samples used to examine the viscosity dependence of kinetic parameters were prepared in 50:50 glycerol– or ethylene glycol–0.01 M KP_i buffer solutions (Douzou, 1974). Samples used to study dimer formation included 2 M NaCl. Anion binding was studied by addition of the appropriate ligand in deoxygenated buffer solution (KCN, Baker; NaN_3, Eastman Kodak; KF, Fisher) to a previously prepared sample. KCN and NaN_3 were added to a 2:1 molar excess per heme; KF was added to ~1 M, as was imidazole. *N*-Ethylmaleimide (NEM) (Sigma) was used to block the β-93 sulfhydryl (SH) by a published procedure (Grassetti & Murray, 1967). The reaction, as followed photometrically at 300 nm, reached completion after several hours. Sulfhydryl reactivity was determined by the method of Ampulski et al. (1969). 4,4′-Dithiobis(pyridine) (4-PDS) (Sigma) was added to the samples and reaction with β-93 SH monitored photometrically at 324 nm.

Methods

Optical Spectroscopy. Optical spectroscopy was initially performed on a Beckman Acta III spectrophotometer and, subsequently, on a Hewlett-Packard 8451 diode array spectrophotometer. The latter was used to prepare computer simulations of absorption spectra of Hb hybrids by summation of spectra obtained for samples of unliganded Hb, metHb, $Fe^{II}(CO)Hb$, and ZnHb. Concentrations of Hb and ZnHb samples were determined according to literature values for extinction coefficients.[2]

Isoelectric Focusing. Isoelectric focusing measurements employed an LKB Multiphor electrofocusing unit. A Model Q-22 Spectroline UV lamp was used to visualize ZnP fluorescence in isoelectric focusing bands. A sample of each fraction and band eluted from the final hybrid purification column was focused according to standard procedure, with analytical Ampholine PAG plates. Three aliquots of each fraction were prepared, one untreated, one reduced with an excess of sodium dithionite (Fisher) and flushed with CO (Matheson) to ensure a homogeneous $Fe^{II}(CO)P$ hybrid solution, and one treated with $K_3Fe(CN)_6$ to detect the presence of FeP subunits; the ZnP subunits remain Zn^{II} under all conditions. These samples were focused along with ZnHb and HbCO as controls.

Large quantities of the oxidized hybrid species also were applied to a preparative-scale Immobiline isoelectric focusing gel, in the presence of $K_3Fe(CN)_6$. The major band, which focused at a p*I* corresponding to that of the oxidized hybrid in an analytical focusing experiment, was isolated from this gel and dispersed into an optical cuvette that contained 0.01 M KP_i buffer, pH 7.0. The optical absorption spectrum of this sample was recorded; a cuvette containing a protein-free slice of the preparative gel dispersed in KP_i was used as a reference.

Determination of FeP and ZnP Content. The pyridine hemochromogen test for porphyrin concentration was used to quantitate ZnP and FeP content of native Hb, ZnHb, and the [Zn,Fe] hybrids. In this procedure, alkaline pyridine is added to a protein sample to extract the metalloporphyrin (Linder et al., 1978), either FeP or ZnP; the addition of dithionite leads to the formation of the $Fe^{II}P(pyr)_2$ complex. In alkaline pyridine, ZnP takes the form $Zn^{II}P(pyr)$. Because dithionite must be added to Hb and hybrid samples, it was added to the ZnHb sample as well, although ZnP is not reduced by dithionite; no effects were observed.

The concentrations of FeP and ZnP in alkaline–pyridine extracts of Hb and ZnHb, respectively, were determined with the extinction coefficients[2] of $Fe^{II}P(pyr)_2$ and ZnP(pyr) and corroborated by comparison to standard solutions of pure FeP and ZnP in alkaline–pyridine. The alkaline–pyridine extracts of the hybrids contain both $Fe^{II}P(pyr)_2$ and ZnP(pyr), and the concentrations of the individual metalloporphyrins were most readily obtained by comparison of the absorbance at selected wavelengths in spectra of the extracts with the absorbance in simulated spectra calculated by summing in fixed proportion the spectra of alkaline–pyridine extracts of Hb and ZnHb. The analysis employed the absorbances of the peaks at 526, 554, and 588 nm and the trough at 574 nm.

The concentration of zinc porphyrin within a hybrid also can be examined by monitoring the ^{3}ZnP formed upon flash photolysis of a hybrid sample (Zemel & Hoffman, 1981). At high intensity of the actinic light, the ZnP can be converted

[2] Extinction coefficients used for optical determination of concentration of components: metHb, $\epsilon_{406} \approx 161$ mM^{-1}; deoxyHb, $\epsilon_{431} \approx 130$ mM^{-1}; HbCO, $\epsilon_{419} \approx 191$ mM^{-1} (Antonini & Brunori, 1971). $Fe^{II}P(pyr)_2$, $\epsilon_{418} \sim 130$ mM^{-1}, $\epsilon_{557} \sim 32$ mM^{-1}, and $\epsilon_{525} \sim 16$ mM^{-1} (Riggs, 1981). ZnHb, $\epsilon_{424} \approx 122$ mM^{-1}; ZnP(pyr), $\epsilon_{425} \sim 126$ mM^{-1}, $\epsilon_{551} \sim 12.3$ mM^{-1}, and $\epsilon_{588} \sim 10$ mM^{-1} (Leonard et al., 1974). [$\alpha(Fe^{III}H_2O)$,β-(Zn^{II})], $\epsilon_{406} \approx 103$ mM^{-1} and $\epsilon_{424} \approx 143$ mM^{-1} (this work). $\Delta\epsilon$(ZnP – ^{3}ZnP; 424 nm) ≈ 80 mM^{-1} (Zemel & Hoffman, 1981). $\Delta\epsilon$(Hb – HbCO; 434 nm) ≈ 95 mM^{-1} and $\Delta\epsilon$(metHb – Hb; 434 nm) ≈ 57 mM^{-1} (Antonini & Brunori, 1971).

quantitatively to ^{3}ZnP; the concentration of ZnP-containing subunits ([ZnP]) was determined from the kinetic absorbance change at $t = 0$ under such conditions.[2] The concentrations determined for ZnHb by this method agree well with those calculated from the ZnHb static absorption spectrum. Similarly, FeP concentrations of a protein sample can be measured from the change in absorbance upon CO binding when the FeP is in the reduced unliganded heme form, with the appropriate changes in extinction coefficient.[2]

^{3}ZnP Decay Measurements. The flash photolysis apparatus for measuring transient absorption changes has been described (Stanford et al., 1980). The actinic sources used were either a Sunpak 611 photographic flash filtered with the appropriate colored glass (Corning 3-71) or an Electrophotonics dye laser (R6G) (emission at 590 ± 10 nm) (Rose & Hoffman, 1983) attenuated with neutral-density filters. The concentration of ^{3}ZnP ([^{3}ZnP]) subsequent to flash excitation of hybrid samples was monitored photometrically at the [$Fe^{III}P$] – [$Fe^{II}P$] difference spectrum isosbestic point, $\lambda \sim 415$ nm, or, in the presence of CO, at the [$Fe^{III}P$] – [$Fe^{II}P(CO)$] isosbestic point, $\lambda \sim 424$ nm. Rates of ^{3}ZnP decay for ZnHb were found to be independent of wavelength so the ^{3}ZnP concentration for ZnHb also was generally measured at 415 nm. The rate constants for ^{3}ZnP decay and the zero-time absorbance change were determined by fitting the time variation of [^{3}ZnP] to an exponential decay; kinetic difference spectra were generated by plotting ΔA_0 over the desired wavelength range. It was possible to vary the fraction f of ZnP that had been excited to the triplet state over the full range, $0 \leq f \leq 1.0$. When more than one ZnP per hemoglobin tetramer is excited to the triplet state, the ^{3}ZnP can undergo quenching by long-range *intra*molecular triplet–triplet energy transfer (Zemel & Hoffman, 1981). This process is eliminated when the fraction of photoexcited ^{3}ZnP is low, $f \leq 15\%$. Thus, unless otherwise stated all the measurements reported here refer to this low-photolysis level, in the absence of energy-transfer processes. Under these conditions, decay traces for all derivatives were shown to be exponential over several (three to five) half-lives.

As will be discussed, photoinitiated electron transfer from ^{3}ZnP to $Fe^{III}P$ within the [$\alpha(Fe^{III}H_2O),\beta(Zn)$] hybrid is accompanied by partial net accumulation of $Fe^{II}P$. To avoid complications from this process, only data from the first few flashes of a given sample were used when monitoring ^{3}ZnP decay rates. The irreversible reduction of $Fe^{III}P$ to $Fe^{II}P$ in the hybrid was monitored kinetically at the [ZnP] – [^{3}ZnP] difference spectrum isosbestic point, $\lambda \sim 434$ nm (Zemel & Hoffman, 1981), with high levels of photolysis. Rates for the formation of $Fe^{II}P$ were determined by fitting the short-time rise of ΔA to a single exponential. From this fit, values for ΔA_∞, the net irreversible change in absorbance, were determined as a function of wavelength, and the kinetic difference spectrum was plotted. These were used to calculate the amount of $Fe^{II}P$ irreversibly formed per flash, by use of known extinction coefficients.[2] A similar experiment was performed in the presence of CO, and the concentration of $Fe^{II}(CO)P$ formed per flash was similarly determined. Samples also were reduced by continuous illumination with an Oriel Corp. Xe–Hg arc lamp screened by an H_2O filter and a Corning 0-52 UV cutoff filter.

Results

Quantitation of Zn,Fe(PPIX). Figure 2 presents the spectra of alkaline–pyridine extracts of the [Zn,Fe] hybrid hemoglobins. The spectra for the two hybrids agree and correlate well with the spectrum generated by summing in 1:1 ratio the spectra of alkaline–pyridine extracts of ZnHb and FeHb. For example, the peak absorbances at 554 and 588 nm primarily represent $Fe^{II}P(pyr)_2$ and ZnP(pyr), respectively, and their ratios are $A(554)/A(558) = 3.1$ for [$\alpha(Fe),\beta(Zn)$], 3.0 for [$\alpha(Zn),\beta(Fe)$], and 3.2 for ZnHb and Hb in 1:1 proportion. In a parallel measurement on a sample of the [Fe^{II},Zn] hybrid, the concentration of ZnP was determined by quantitation of ^{3}ZnP formation upon photolysis, and that of FeP was determined by quantitation of the spectral change observed upon reaction with CO. Within the limits of experimental error (±10%), these results also indicate a 1:1 ratio of ZnP:FeP in the hybrid.

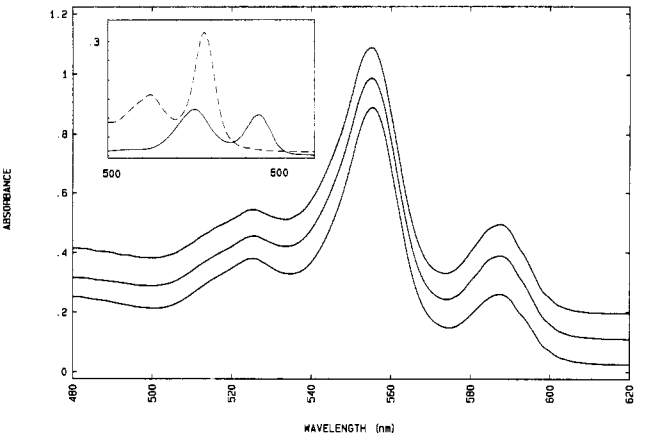

FIGURE 2: Absorption spectra of the alkaline–pyridine extracts of the [Zn,Fe] hybrids. Conditions: 20% (0.01 M KP_i, pH 7.0), 80% (1/3 v/v pyridine/H_2O, 0.1 N NaOH); ~3 μM hybrid tetramer. (A) [$\alpha(Zn),\beta(Fe)$]. (B) [$\alpha(Fe),\beta(Zn)$]. (C) A computer simulation of a spectrum of 1:1 contribution from the reduced pyridine hemochromogen extracts of ZnHb:FeHb. Note: A subtraction of C from either A or B is featureless. (Inset) Reference spectra for the extracts of equal concentrations of ZnHb (—) and of Hb (--).

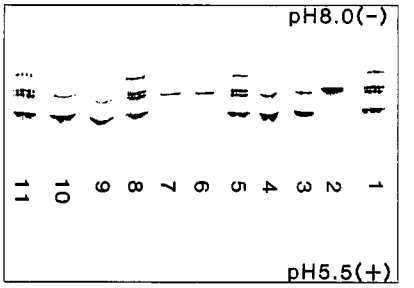

FIGURE 3: Isoelectric focusing of the [$\alpha(Fe),\beta(Zn)$] hybrid, HbCO, and ZnHb. Top of figure, cathode (–), pH 8.0; bottom of figure, anode (+), pH 5.5. (Lanes 1, 5, 8 and 11) HbCO control. (Lane 2) ZnHb. (Lanes 3 and 4) [$\alpha(Fe),\beta(Zn)$] hybrid as isolated from DEAE column. (Lanes 6 and 7) Chromatographed [$\alpha(Fe),\beta(Zn)$] hybrid, subsequently treated with $K_3Fe(CN)_6$. (Lanes 9 and 10) Chromatographed [$\alpha(Fe),\beta(Zn)$] hybrid treated with dithionite and flushed with CO. Note a small band of excess oxidized hybrid due to incomplete reduction. See text for preparation and discussion.

Isoelectric Focusing of [Fe,Zn] Hybrids. The focusing patterns for the [$\alpha(Fe),\beta(Zn)$] hybrids and the HbCO and ZnHb controls are presented in Figure 3. The [$\alpha(Zn),\beta(Fe)$] hybrid behaves in a similar fashion and is not shown. Lanes 1, 5, 8, and 11 show the pattern for HbCO while lane 2 shows that for ZnHb. Lanes 3 and 4 show the untreated hybrid taken directly from the purification column. Lanes 6 and 7 are the oxidized hybrid. Lanes 9 and 10 are the hybrid reduced and exposed to CO. The bands for ZnHb and for the [Zn,Fe] hybrids fluoresce, confirming the presence of ZnP. The bands for the hybrids fluoresce to a lesser extent than ZnHb due to the presence of FeP.

For HbCO, in lanes 1, 5, 8, and 11, four bands are seen. The major band lies closest to the anode and represents HbCO

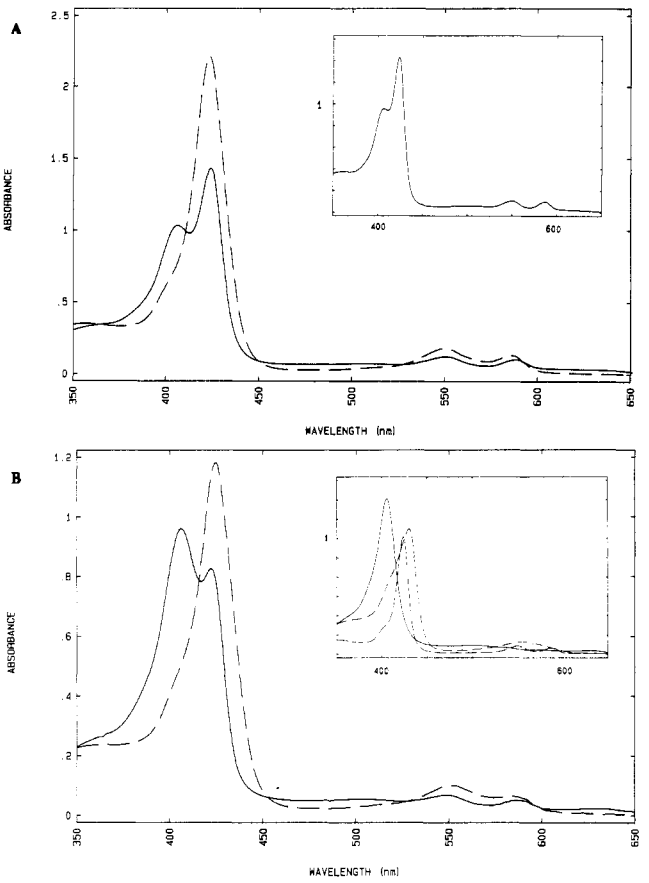

FIGURE 4: Absorption spectra of the oxidized and reduced forms of the [Zn,Fe] hybrids and Hb. Conditions: 0.01 M KP_i, pH 7.0, ambient temperature. (A) [$\alpha(Fe^{III}H_2O),\beta(Zn^{II})$] (—); [$\alpha(Fe^{II}),\beta(Zn^{II})$] (--). (Inset) [$\alpha(Fe^{III}H_2O),\beta(Zn^{II})$] obtained directly from the oxidized band of an isoelectric focusing gel (—). (B) computer simulation of the oxidized and reduced forms of the hybrids prepared by summing, 1:1, spectra normalized to the same concentration of ZnHb + metHb (—) and ZnHb + deoxyHb (--). (Inset) MetHb (—); deoxyHb (--); ZnHb (-·-).

([$\alpha(Fe^{II}CO),\beta(Fe^{II}CO)$]) ($P_1 \sim 7.2$). The fully oxidized hemoglobin species, [$\alpha(Fe^{III}),\beta(Fe^{III})$], lies closest to the cathode ($P_1 \sim 7.6$). Half-oxidized, valency hybrid hemoglobins [$\alpha(Fe^{II}CO),\beta(Fe^{III})$] and [$\alpha(Fe^{III}),\beta(Fe^{II}CO)$] are visible as two bands that focus midway between the fully oxidized and fully reduced proteins.

The [Zn^{II},Fe^{III}] oxidized hybrids, whose focusing pattern is shown in lanes 6 and 7, are analogous to valency hybrids and focus at the valency hybrid position, as expected. The major band observed in the untreated hybrid (lanes 3 and 4) falls at the position of HbCO and corresponds to the fully reduced form, [$Zn^{II},Fe^{II}(CO)$]; the band at the valency hybrid position in these samples is due to partial oxidation of the hybrid during purification. This assignment is confirmed by reaction of the hybrid with dithionite and CO (lanes 9 and 10), which reduces the relative intensity at the valency hybrid position and increases that of the fully reduced hybrid. Likewise, oxidation of the hybrid diminishes the fully reduced band and increases that at the valency hybrid position (lane 4). Note that no bands due to α or β chains or semiglobin were observed in the hybrid, nor is there contaminating native Hb. The latter would have appeared as a band at the position of fully oxidized Hb when the hybrid sample was oxidized.

Optical Spectra of [Zn,Fe] Hybrids. Figure 4 presents the optical spectra of the [$\alpha(Fe),\beta(Zn)$] hybrid in its reduced, [Zn,Fe^{II}], and oxidized, [$Zn,Fe^{III}H_2O$], states as well as the absorption spectrum of the hybrid isolated from a preparative isoelectric focusing gel. Oxidized hybrid, [$\alpha(Fe^{III}H_2O),\beta(Zn)$], applied to this gel focused into one major band at the p*I* corresponding to that observed for the oxidized hybrid in an analytical focusing experiment.[3] This band was isolated and dispersed into KP_i buffer. Its absorption spectrum is the same as that of the solution before application to the gel, and thus we conclude that the hybrid is a homogeneous protein, uncontaminated by excess ZnHb or reduced hybrid, both of which focus at separate positions from that of the oxidized hybrid.

The extensive efforts to verify the stoichiometry and homogeneity of the hybrid were prompted by the following observations. The ratio of the absorbance at the Soret peak maximum of metHb (λ = 406 nm; Antonini & Brunori, 1971) to that at the Soret maximum of ZnHb (λ = 424 nm; Leonard et al., 1974) in the oxidized [$\alpha(Fe^{III}),\beta(Zn)$] hybrid is $R \equiv A(424)/A(406) \sim 0.72$. This value is not altered by further incubation of the hybrid for 8 h in the presence of a 1.5-fold excess of oxidant. The spectrum for the corresponding $\alpha(Zn)$ hybrid is almost identical, but with $R \sim 0.67$. However, in a computer-simulated spectrum prepared by adding 1:1 contributions from ZnHb and metHb (Figure 4B), $R \sim 1.1$, much larger than that for the hybrids. Thus, although the spectra of reduced and oxidized hybrids qualitatively resemble the superposition of a spectrum of ZnHb with those of ferrous Hb and aquomet Hb (Figure 4B), respectively, the spectra of the oxidized hybrids are not reproduced quantitatively by 1:1 superposition. The most obvious explanation of this discrepancy would be an excess of ZnP associated with the protein. However, this is ruled out by the quantitations described above. To reproduce the experimental value of R would require a ZnP:FeP ratio of 2.5:1. But this proportion would give a pyridine hemochromogen spectrum incompatible with that observed (Figure 2) with, for example, the low value of $A(554)/A(588) = 2.0$.

Since there is little difference between the Soret peak maxima of the ZnP, deoxy-$Fe^{II}P$, and $Fe^{II}(CO)P$ in the hybrid, the apparent discrepancy in the spectra of the [Fe^{III},Zn] hybrids could result from incomplete oxidation and the resulting presence of partially reduced or CO forms of the hybrid. In fact, it has been shown that the procedure used to oxidize the proteins with $K_3Fe(CN)_6$ can leave a small fraction of the sample reduced (Linder et al., 1978), and this is sometimes evident as a weak band at the position of the fully reduced Hb upon isoelectric focusing of oxidized hybrid. However, simulations show that to reproduce a ratio $R \sim 0.72$ would require ~50% of the hemes to be in the unliganded $Fe^{II}P$ form or 40% in the CO form; even greater fractional reduction is necessary to mimic the $R \sim 0.67$ for the [$\alpha(Zn),\beta(Fe^{III}H_2O)$] hybrid. This explanation is incompatible with the equivalence of optical spectra for focused and unfocused [$\alpha(Fe^{III}H_2O),\beta(Zn)$] hybrid (Figure 4A). Most importantly, upon flash photolysis of an oxidized hybrid sample there is no kinetic absorption change that could be attributed to photolysis of $Fe^{II}(CO)P$ present in the sample. Neither is there a change in the spectrum upon exposure of the oxidized hybrid to 1 atm of CO. Therefore, the spectrum of the oxidized hybrid has no significant contribution from any reduced species. We conclude that the optical spectra are representative of pure, homogeneous

[3] Some smearing of the protein was observed as well as a minor band at the position of fully reduced hybrid. These features are most likely due to a small amount of reduction or denaturation of the protein during the lengthy focusing procedure. However, the preparative-scale Immobiline IEF gel can separate components as close as 0.1 pH unit, and the major band of protein was isolated from all other components.

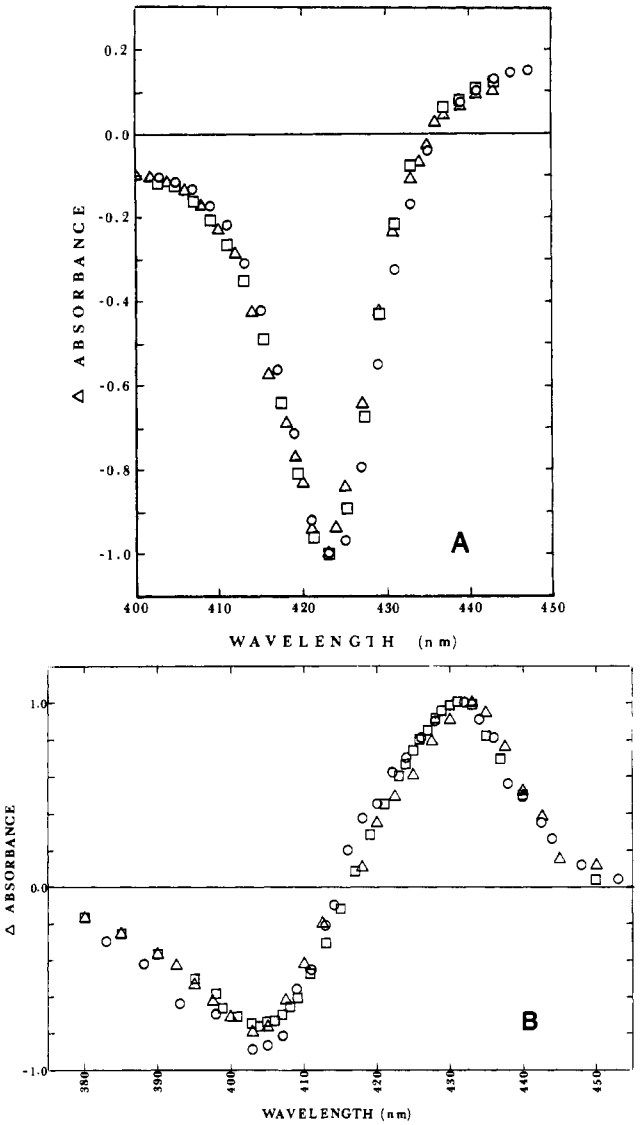

FIGURE 5: (A) Kinetic difference spectra of ΔA_0 (absorbance units) for various [α(Fe),β(Zn)] derivatives (Note the virtually identical isosbestic points and peak maxima): (□) [α(Fe^{II}),β(Zn)]; (○) [α($Fe^{III}H_2O$),β(Zn)]; (△) [α($Fe^{III}CN^-$),β(Zn)] as a representative anion-bound species. (B) Static difference spectra for the [α(Fe),β(Zn)] hybrid and Hb. (△) Difference between [α(Fe^{III}),β(Zn)] and the $\alpha(Fe^{II})$ form obtained by prolonged irradiation. (□) MetHb – deoxyHb difference spectrum prepared by recording a spectrum of metHb, reducing the sample with dithionite, recording a second spectrum, and subtracting it from the first. (○) Kinetic difference spectrum of the persistent spectral change generated by high intensities of the actinic light. Isosbestic point ~415 nm; ΔA^+_{max} ~432 nm; ΔA^-_{max} ~405 nm. Sample conditions as in Figure 4.

[$Fe^{III}(H_2O)$,Zn] hybrids and that the apparent discrepancy between observed and predicted spectra represents a perturbation in the spectrum of the $Fe^{III}P$ chains reflective of the incorporation of a liganded (six-coordinate) $Fe^{III}(H_2O)P$ into a Hb tetramer in the "deoxy", T quaternary state (Blough et al., 1980). Such differences are well-known in the study of valency hybrids (Bannerjee & Cassoly, 1969; Brunori et al., 1970; Matawari et al., 1983). The T-state [Zn,$Fe^{III}(H_2O)$] hybrid appears to exhibit these effects to a unique degree, presumably because the $Fe^{III}(H_2O)P$ is more sensitive to the structural perturbations caused by incorporating a subunit with a liganded heme into a tetramer in the unliganded (T) quaternary structure (Arnone et al., 1986).

^{3}ZnP Decay Kinetics. Both [α(Fe),β(Zn)] and [α(Zn),β(Fe)] hybrid hemoglobins were employed in the flash photolysis studies. No difference in ^{3}ZnP decay kinetics was observed at ambient temperature, but the [α(Zn),β($Fe^{III}H_2O$)] hybrid undergoes slow autoreduction and therefore is less convenient to use. Therefore, we discuss only the [α(Fe),β(Zn)] hybrid, except insofar as the properties of the [α(Zn),β(Fe)] species that differ. Measurements on the latter were made immediately after sample preparation, to avoid autoreduction.

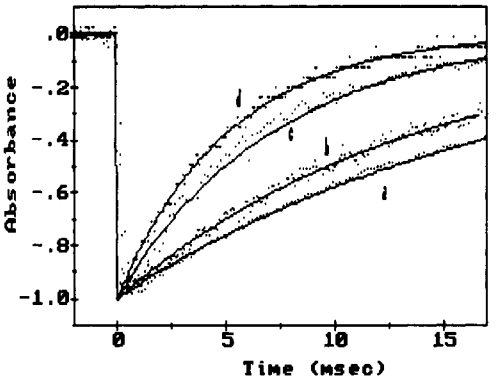

FIGURE 6: Normalized progress curves of the ^{3}ZnP decay subsequent to flash photolytic excitation of [α(Fe),β(Zn)] hybrid hemoglobins, as monitored through the ZnP – ^{3}ZnP difference spectrum at 415 nm and the isosbestic point of the $Fe^{III}P$ – $Fe^{II}P$ difference spectrum. Solid curves represent the results of a nonlinear least-squares fit to an exponential; rate constants averaged over numerous such traces are given in Table I. Conditions: 0.01 M KP_i, pH 7.0; [IHP] = 30 μM; ambient temperature; [tetramer] ~ 3 μM. (a) (Lowest curve) [α(Fe^{II}),β(Zn)]. (b) [α($Fe^{III}CN^-$),β(Zn)]. (c) [α($Fe^{III}(H_2O)$),β(Zn)]. (d) [α(Fe^{III}imid),β(Zn)].

Intrahybrid Quenching of ^{3}ZnP by $Fe^{II}P$. The kinetic difference spectra (Figure 5) obtained from flash photolysis experiments using low levels of photolysis for both reduced [α(Fe^{II}),β(Zn)] and oxidized [α(Fe^{III}),β(Zn)] hybrid species are indistinguishable from the [ZnP] – [^{3}ZnP] difference spectrum of ZnHb (Zemel & Hoffman, 1981), with no detectable contribution from the aquoferriheme. At the low levels of photolysis employed to prevent ^{3}ZnP–^{3}ZnP energy transfer, the rates of ^{3}ZnP decay observed were first order and invariant across the spectrum.

Figure 6 presents the progress curves for the decay of the ^{3}ZnP produced by flash excitation in the [Zn,Fe] hybrid hemoglobins at ambient temperature. The upper curve results from the ^{3}ZnP decay in the reduced hybrid, in which the heme is in the high-spin, $Fe^{II}P$, state ([α(Fe^{II}),β(Zn)]). Triplet decay is not enhanced by the presence of ferroheme within the hybrid, for the decay rate, $k_D = 50 \pm 3\ s^{-1}$, is similar to that for ^{3}ZnP in an individual subunit of fully substituted ZnHb (Zemel & Hoffman, 1981). However, when the hybrid contains the aquoferriheme, $Fe^{III}P$, the ^{3}ZnP decay remains a single exponential, but the rate is much greater, $k_{obsd} = 150 \pm 10\ s^{-1}$ (Figure 6). The rate at which the aquoferriheme in the [Zn,Fe] hybrid quenches the ^{3}ZnP, k_t, is the difference between the ^{3}ZnP decay rates in the ferri- and ferroheme hybrids

$$k_t = k_{obsd} - k_D = 100\ s^{-1}$$

and the quantum yield for quenching is

$$\phi_t = \frac{k_t}{k_D + k_t} \sim \frac{2}{3}$$

As may also be seen in Figure 6 and Table I, the quenching rate is quite sensitive to the ferriheme ligation state. A major element of this paper is a demonstration that this quenching process represents long-range intramolecular ^{3}ZnP → $Fe^{III}P$ electron transfer.

Variation in hybrid concentration from 5 to 35 μM in heme has no effect on the observed rates of ^{3}ZnP decay. Nor does

Table I: Observed Rates of ^{3}ZnP Decay (k_{obsd}) and of Electron Transfer (k_t)[a] for Various [Zn,Fe] Hybrid Derivatives[b]

derivative	k_{obsd} (s^{-1})	k_t (s^{-1})
[Zn,Fe^{II}]	50 (3)	0 (3)
[Zn,Fe^{II}(CO)]	50 (3)	0 (3)
[Zn,Fe^{III}(imidazole)]	225 (15)	175 (15)
[Zn,$Fe^{III}(H_2O)$]	150 (10)	100 (10)
[Zn,$Fe^{III}(CN^-)$]	70 (5)	20 (5)
[Zn,$Fe^{III}(F^-)$]	70 (5)	20 (5)
[Zn,$Fe^{III}(N_3^-)$]	70 (5)	20 (5)

[a] $k_D = 50\ s^{-1}$; $k_t = k_{obsd} - k_D$. Reported rate constants are averages over measurements on numerous samples. [b] Solutions prepared as described under Methods; conditions as in Figure 4; ambient temperature ($T \sim 22$ °C). Uncertainties in last place(s) are given in parentheses.

the ~6-fold increase in viscosity caused by the addition of glycerol to 50% (v/v, 0.01 M KP_i; Douzou, 1974). Neither is the ^{3}ZnP decay of ZnHb influenced by the addition of an equimolar amount of metHb to a ZnHb solution. Together, these experiments show that ^{3}ZnP within an [Fe^{III},Zn] hybrid is quenched by the Fe^{III}P in an *intramolecular* process. Because IHP is present in the samples studied, we know from our earlier studies (Blough et al., 1980) that the quenching is associated with tetrameric hybrid in the T (deoxy) quaternary structure. However, results obtained in the pH 7.0, 10 mM KP_i buffer are not dependent on the presence of IHP, consistent with the conclusion that the T state is intrinsically favored under these conditions.

Quenching Is Associated with $^3ZnP \rightarrow Fe^{III}P(H_2O)$ Electron Transfer. Careful comparisons of static absorption spectra of [$\alpha(Fe^{III}H_2O)$,β(Zn)] hybrid samples taken before and after CW or multiple-flash photolyses show a small net Fe^{III}P reduction that is not observed for metHb, [ZnHb], [α(Zn),$\beta(Fe^{III}H_2O)$], or the [Fe^{II},Zn] hybrids. The photolysis-generated static difference spectrum for the [$\alpha(Fe^{III}H_2O)$,β(Zn)] hybrid (shown in Figure 5) correlates closely to the metHb – deoxyHb difference spectrum; no contribution from a change in the spectrum of ZnP is detected. Progressive photoreduction of aquoferriheme is paralleled by a decrease in the rate of ^{3}ZnP decay until the hybrid is fully reduced to the [Zn,Fe^{II}P] state and k_{obsd} has returned to the corresponding rate: $k_{obsd} \rightarrow k_D = 50\ s^{-1}$. The observation of irreversible reduction unambiguously confirms that the quenching of ^{3}ZnP in the [$\alpha(Fe^{III}H_2O)$,β(Zn)] hybrid involves $^3ZnP \rightarrow Fe^{III}P$ electron transfer.

As yet, measurements on the [Zn,Fe] hybrids with low levels of ^{3}ZnP formation ($f \lesssim$ 10–15%) have shown no direct kinetic manifestation of heme reduction; the kinetic difference spectrum is dominated by ^{3}ZnP and the transient absorbance signal decays exponentially to base line. However, when [$\alpha(Fe^{III}H_2O)$,β(Zn)] is illuminated with higher intensity flashes ($f \rightarrow 1$), the ^{3}ZnP transient decays to a new, persistent base-line level. A kinetic difference spectrum obtained by plotting this persistent spectral change is indistinguishable from that observed for the [Fe^{III}P] – [Fe^{II}P] difference spectrum measured upon reduction of metHb to the deoxyHb form (Figure 5B). This signal is not observed for the [α(Zn),$\beta(Fe^{III}H_2O)$] or [Zn,Fe^{II}] hybrids or ZnHb: All kinetic transients observed with these proteins, even at high levels of photolysis, decay to base line. Moreover, metHb shows no kinetic transients on the time scale of these measurements. The kinetic formation of Fe^{II}P subsequent to flash excitation of [$\alpha(Fe^{III}H_2O)$,β(Zn)] hybrid was monitored at the ZnP–^{3}ZnP isosbestic point, λ = 434 nm (Zemen & Hoffman, 1981), under high levels of photolysis. The very low intensity of this signal and the presence of a second, small and unrelated transient signal at the ZnP–^{3}ZnP isosbestic point makes analysis difficult, but the rate of formation of the Fe^{II}P is very similar to k_t, as expected for electron transfer from ^{3}ZnP.

Since repeated flashes or prolonged photolysis of the aquomet hybrid sample ultimately cause reduction of the aquoferriheme, whereas a metHb sample treated identically is not reduced, this net photoreduction of the aquoferriheme must result from electron transfer from ^{3}ZnP in the adjacent subunit, according to the kinetic scheme illustrated in Figure 1. The accumulation of Fe^{II}P indicates that, in addition to the thermal electron-transfer process, there is an alternate decay channel for the [$ZnP^{\bullet+}$,Fe^{II}P] intermediate, one in which $(ZnP)^+$ is reduced by solution impurities or an as-yet-unidentified protein residue; we define the rate-constant for this process as k_m. The amount of Fe^{II}P formed per flash was determined from the net change in absorbance at the ZnP – ^{3}ZnP isosbestic point. Comparison of this value to the concentration of photoinitiated ^{3}ZnP formed per flash of the same intensity indicates that the irreversible reduction of Fe^{III}P occurs with a quantum yield of $\phi_m = 0.24$ per ^{3}ZnP formed.

Subsequent reoxidation of the photoreduced hybrid produces an aquoferriheme derivative whose absorption spectrum is identical with that of freshly prepared protein, and the difference spectrum generated by subtraction also mimics the metHb – deoxyHb spectrum. As ZnP makes no apparent contribution to the static difference spectrum, the ZnP appears to be unaltered by the photoreduction (and reoxidation) processes. Moreover, the process leading to net accumulation of Fe^{II}P under illumination does not appear to affect protein residues essential to the integrity of the hybrid or to the electron-transfer process. Samples that had been completely photoreduced and then reoxidized were subject to a second prolonged illumination. This resulted in photoreduction of the Fe^{III}P for the second time, in roughly the same period of illumination.

One possible explanation for the net reduction of Fe^{III}P upon irradiation of [$\alpha(Fe^{III})$,β(Zn)] is that the strongly oxidizing $(ZnP)^+$, zinc–porphyrin π-cation radical formed by the photoprocess is reduced by a nearby protein residue. This would return the neutral ZnP state without reoxidizing its ferroporphyrin partner, thereby trapping the heme in the Fe^{II} state. Because the [α(Zn),$\beta(Fe^{III}H_2O)$] hybrid does not exhibit a net photoreduction, a plausible candidate for the reductant of $(ZnP)^+$ in the β subunit is the sulfhydryl from cysteine residue β-93 (F9). However, titration of β-93 with PDS gives the expected stoichiometry of 1.0 (1) per β-subunit both before and after complete photoreduction of the hybrid. Furthermore, in separate experiments, the β-93 SH was first blocked by reaction with NEM, and this did not alter the ^{3}ZnP decay rates, nor did it change the rate of accumulation of Fe^{II}P upon photolysis. Thus, β-93 appears not to be involved.

The [ZnP] – [^{3}ZnP] difference spectrum also was examined in case the alteration of an amino acid residue near the heme might exert an observable effect. Careful observation of the [ZnP] – [^{3}ZnP] kinetic difference spectrum during gradual photoreduction of the [Zn,Fe] hybrid reveals a concurrent red shift in its isosbestic point. Reoxidation of a completely photoreduced sample returns the isosbestic point to its original value, which implies that the effect is associated with photoreduction but is not due to chemical modification of ZnP. For reasons discussed below it is important to note that the ^{3}ZnP decay rate, k_D, is the same for fully photoreduced hybrid as for a chemically reduced sample, despite the shift in isosbestic point.

^{3}ZnP Decay in Ligated Hybrid Derivatives. Figure 6 presents ^{3}ZnP decay curves for various hybrid derivatives, and

Table II: Comparisons of Relative Rates of Triplet-State Electron Transfer (k_t) with Predictions for Relative Rates of Energy Transfer (k_E) for Various [α(Fe),β(Zn)] Hb Hybrid Derivatives

derivative	measured[a] $k_t/k_t(Fe^{III}(H_2O))$	theory[b] $k_E/k_E(Fe^{III}(H_2O))$
[Zn,Fe^{II}]	0	0.9
[Zn,Fe^{II}(CO)]	0	0
[Zn,$Fe^{III}(H_2O)$]	1.0[a]	1.0[a]
[Zn,$Fe^{III}(CN^-)$]	0.2	0.1
[Zn,$Fe^{III}(F^-)$]	0.2	3.1

[a] Rate ratios are relative to that for the [$\alpha(Fe^{III}H_2O)$,β(Zn)] hybrid; data from Table I. [b] Relative energy-transfer rates calculated, as described in text, as the ratio of the spectral overlap integral for a given derivative to that for the [Zn,$Fe^{III}(H_2O)$] is $I = 1.04 \times 10^{-11}$ cm^6 mol^{-1}.

a summary of the decay rates is presented in Table II. The decay rate for the Fe^{II}(CO)P derivative is identical with that observed for the Fe^{II}P derivative. Although the CO is photolabile, very low levels of actinic light were employed, with less than 10% of the CO being expelled. Thus more than 90% of the ^{3}ZnP is associated with the [^{3}ZnP,Fe^{II}P(CO)] species, and the rate of ^{3}ZnP decay is indeed associated with that derivative and not with the [^{3}ZnP,Fe^{II}P] hybrid formed by expulsion of CO.

The rates of ^{3}ZnP decay observed for the ferriheme derivatives formed by binding the anions F^-, N_3^-, and CN^- are indistinguishable and significantly less than that observed for the aquoferriheme derivative. In contrast, the ^{3}ZnP decay rate is much larger in the imidazole derivative. The cyanomet derivative was further characterized as a representative anion-ligated hybrid species. The [ZnP] − [^{3}ZnP] kinetic difference spectrum mimics that of ZnHb (Figure 5A). Most importantly, the observation of net reduction of the cyanoferriheme confirms the occurrence of electron transfer.

Are There Quenching Mechanisms Other Than Electron Transfer? The triplet quenching yield within the [α-($Fe^{III}H_2O$),β(Zn)] hybrid has a value of $\phi_t = 100/(100 + 50) = 0.67$; of that, the component representing net photoreduction is $\phi_m = 0.24$. We must now show that the triplet quenching is entirely the result of electron transfer, for the incomplete net photoreduction ($\phi_m < \phi_t$) admits the possibility that alternate intramolecular quenching processes are operative. These could have a yield of as high as 0.43, and thus, the experimental bounds on the electron-transfer rate constant are $100 > k_t > 37$ s^{-1}. We shall discuss in turn the three alternate mechanisms that must be considered and in so doing show that *none* makes a significant contribution. Rather, we conclude that within experimental error the quenching occurs solely by electron transfer, that $k_t = 100$ (± 10) s^{-1}, and that the incomplete net reduction results from a competition between reverse electron transfer (rate constant, k_b; Figure 1) and net reduction (rate constant, k_m). According to our kinetic scheme, as expanded to include the net reduction, this is equivalent to saying that the electron-transfer process $Fe^{II}P \rightarrow ZnP^+$ has a quantum efficiency ϕ_b and irreversible reduction has an efficienty ϕ_m with values of

$$\phi_b = \frac{k_b}{k_b + k_m} = 0.76 \qquad \phi_m = \frac{k_m}{k_b + k_m} = 0.24$$

and with $k_b/k_m \sim 3$.

The first alternate mechanism, paramagnetic quenching of ^{3}ZnP, might be operative in either the Fe^{II} or Fe^{III} hybrids. Considering the former, the ferrous, unliganded Fe^{II}P of the [Zn,Fe^{II}] hybrid species is high spin, $S = 2$; the ferrous CO hybrid derivative [Zn,Fe^{II}(CO)] is low spin, $S = 0$. However, k_D for the ^{3}ZnP is the same in the two derivatives (Table II). This result shows that paramagnetic quenching of ^{3}ZnP by Fe^{II}P in the ferrous, unliganded hybrid derivative is unimportant.

Both the aquo- and fluoroferriheme hybrid derivatives are high spin, $S = {}^5/_2$, and would be expected to behave similarly if spin quenching is important. However, the fluoroferriheme hybrid has a much slower rate of ^{3}ZnP decay (Table II), similar to that of the low-spin, cyanomet species ($S = {}^1/_2$) and the azidomet species, which is a mixture of spin states (Antonini & Brunori, 1971). Therefore, paramagnetic quenching of the ^{3}ZnP by the aquoferriheme does not contribute to the increase in the rate of ^{3}ZnP decay observed upon oxidation of the hybrid.

A second, more plausible, alternate is that the ^{3}ZnP is quenched by Förster-type long-range dipole–dipole energy transfer from ^{3}ZnP to its partner FeP. This process would be analogous to the triplet–triplet transfer we studied in ZnHb (Zemel & Hoffman, 1981) and is sensitive to the distance, orientation, and spectral overlap of the donor–acceptor pair. Its rate constant, k_E, can be described by

$$k_E \propto \frac{K^2}{n^4 \tau R^6} I$$

where $I = \int F_D(\lambda)\epsilon_A(\lambda)\lambda^4 \, d\lambda$ is the spectral overlap integral between the normalized donor emission spectrum, $F_D(\lambda)$, and the acceptor absorbance spectrum, $\epsilon_A(\lambda)$, described by the molar absorptivity, R is the α_1–β_2 interchromophoric distance ($R = 25$ Å for the Zn–Fe distance), τ is the natural radiative lifetime of the donor emission, n is the refractive index of the medium, and K^2 is a dipole–dipole orientation factor (Conrad & Brand, 1978). For the [Zn,Fe] hybrid hemoglobins, the presence of IHP in all sample solutions ensures that all of the tetramers are fixed in the T (deoxy) conformation. Thus, the only variables that change with the state of the FeP are K^2 and the spectral overlap integral.

Eaton et al. have shown that there are contributions to the FeP absorption spectra from in-heme plane transitions in each of the derivatives studied here (Eaton et al., 1978; Eaton & Hofrichter, 1981); since the α_1–β_2 hemes are roughly parallel in the T-state tetramer, K^2 is nonzero (Dale et al., 1979). In the standard way, we may estimate k_E using the upper limit of $K^2 = 1$ (Turro, 1978). In this case, the ratio of spectral overlap integrals for the different hybrid forms should closely approximate the ratio of energy-transfer rates. The overlap integral for each of the hybrid forms examined was calculated from spectra of Hb derivatives to represent the hybrid's ligated FeP subunits (Eaton & Hofrichter, 1981; Antonini & Brunori, 1971); the normalized ZnHb phosphorescence spectrum was used to represent the ^{3}ZnP emission spectrum.[4] The relative values for integrals, and thus k_E, for the various [Zn,Fe] hybrid derivatives are listed in Table II as ratios to the value for the aquomet hybrid.

The overlap integral for the [Zn,Fe^{II}(CO)] hybrid is essentially zero, ca. 40-fold less than for the unliganded Fe^{II} derivative, yet both exhibit the same, slow rate of ^{3}ZnP decay. This result demonstrates that there is no energy-transfer contribution to k_D for the [Zn,Fe^{II}] reference state. The calculation of overlap integrals predicts that the relative rate of ^{3}ZnP quenching by energy transfer from ^{3}ZnP to FeP should be very similar for the [Zn,$Fe^{III}(H_2O)$] and [Zn,Fe^{II}] hybrids, yet for the former $k_t = 100$ s^{-1} and for the latter $k_t = 0$. The fluoroferriheme hybrid is predicted to have an energy-transfer

[4] G. Yanowitch and B. M. Hoffman, unpublished results.

rate 3 times as large as that for the aquomet species, yet the quenching rate is only 15% as large. These discrepancies between the predicted rates of energy transfer and the experimental values of k_t indicate that energy transfer does not contribute to the ^{3}ZnP quenching.

The third potential mechanism to address[5] is the possibility that minor differences in electronic and vibrational structure among the various hybrids might affect the nonradiative decay of ^{3}ZnP, thereby changing the value of k_D. As the solution conditions have been chosen so that all forms of the hybrid adopt the T-state quaternary structure, the question can be rephrased as follows: does a change in the ligation state of FeP in the $\alpha(\beta)$ chain perturb the ZnP in the $\beta(\alpha)$ chain, in the absence of an accompanying change of quaternary structure.[6]

Years of spectroscopic study of Hb hybrids have shown that such a direct interaction among heme sites does not occur (Perutz, 1979; Bunn & Forget, 1986). Indeed, our X-ray diffraction study of the T state, [α(FeCO),β(Mn^{II})] hybrid clearly demonstrates that the five-coordinate β(Mn^{II}P), which is a close structural analogue of the five-coordinate Fe^{II}P and Zn^{II}P, is not perturbed by ligation of the α(FeP). Rather, the X-ray structure visualizes what was spectroscopically anticipated, that the environment of a ligated FeP within a T-state tetramer differs notably from that within the R- ("oxy") state tetramer. This perturbation causes the anomaly in the optical spectrum of the six-coordinate Fe^{III}(H$_2$O)P-containing chains of the hybrids, whereas the spectra of the five-coordinate ZnP chain are normal, despite the fact that they would be sensitive to environmental perturbations.

Direct confirmation that this mechanism makes no significant contribution comes from the measured invariance of k_D. It is the same for ZnP within the slightly different environments of the α(Zn) and β(Zn) hybrids. In both hybrids it is the same in the totally unliganded [Zn,Fe^{II}] form, where there is no "mismatch" between FeP ligation state and protein T quaternary structure, and in the diliganded, T-state (Zn,Fe(CO)] form, where the mismatch is maximal (Table I). Thus, k_D for ZnP incorporated within the T-state tetramer can be treated as a single, essentially invariant parameter.

The above considerations all lead us to conclude that ^{3}ZnP quenching within the [Zn,Fe^{III}(H$_2$O)] hybrids is not significantly attributable to any of the alternate mechanism, and that the quenching rate of k_t = 100 ($\pm$10) s^{-1} is, within experimental error, attributable solely to ^{3}ZnP $\rightarrow$ Fe^{III}P electron transfer. The rate constant, k_t, depends strongly on the heme ligation state (Table I). The same considerations indicate that the increased value of k_t for the imidazole-bound hybrid also, within error, is solely representative of electron transfer and that the electron-transfer rate is greatly reduced by anion (F^-, CN^-, N_3^-) binding. In the anion-bound forms, the quenching rate is so small that it is possible that some percentage of this residual might be ascribable to an alternate mechanism, in which case the decrease in electron-transfer rate is even greater than apparent. However, even here, the observation of net photoreduction with the CN^- derivative demonstrates electron transfer.

Estimates of k_b and k_m. Because carbon monoxide will bind to Fe^{II}P but not to Fe^{III}P and does not alter the rate of ^{3}ZnP decay, the electron-transfer experiments were performed in the presence of high CO concentrations, in the hope of augmenting the degree of net heme reduction. Binding of CO to the flash-produced ferroheme might be expected to compete with the reverse electron-transfer process:

$$Fe^{II}P + CO \xrightarrow{k_{CO}} Fe^{II}P(CO)$$

In the presence of IHP, the hybrid is fully T state, and CO binding to the ferroheme with 1 atm of CO is pseudo first order and monophasic: $k_{CO}^T = 10^2$ s^{-1} (Blough et al., 1981). Careful measurement of the amount of Fe^{II}P(CO) formed per triplet shows that the presence of 1 atm of CO does not significantly increase the amount of Fe^{II}P formed per flash. From this we may conclude only that $k_b \gg k_{CO}^T$ or $k_b \gg 100$ s^{-1}. In the absence of IHP, the hybrid tetramer is partially R state and binds CO with a rate of $k_{CO}^R \sim 5 \times 10^3$ s^{-1} (Blough et al., 1981). Experiments performed under these conditions also show no increase in net Fe^{II}P production. The result is suggestive that $k_b \gtrsim k_{CO}^R \sim 5 \times 10^3$ s^{-1}. Such a value of k_b is consistent with a failure to observe directly the transient intermediate that results from ^{3}ZnP $\rightarrow$ Fe^{III}P electron transfer. By the kinetic scheme of Figure 1, the maximum concentration (I_{max}) for this intermediate would be exceedingly small compared to the initial ^{3}ZnP concentration ($^*A_0$): $I_{max}/{}^*A_0 \sim k_t/k_b \sim 10^{-3}$. Our observation that $k_b \gg k_t$ parallels the direct observation of such an inequality in the complex between Zn-substituted yeast cytochrome *c* peroxidase and yeast cytochrome *c* (Liang et al., 1986).

Support for Assigning (α_1,β_2) as the Primary Electron-Transfer Unit. We have naturally assumed that the functioning electron-transfer unit within the T-state, [Zn,Fe] hybrid Hb tetramer is the unit of closest metal–metal approach (25 Å), the (α_1,β_2) pair (Fermi & Perutz, 1981). This rests on the well-founded expectation that electron transfer would be much slower at the longer (37 Å) separation between redox centers of the (α_1,β_1) dimer (Mayo et al., 1986). However, because the effects of specific amino acid residues that may lie in that pathway are unknown, experimental corroboration was sought. High salt concentrations are known to promote the dissociation of tetramers into (α_1,β_1) dimers (Kirshner & Tanford, 1964). Thus, electron-transfer measurements were performed with [Zn,Fe] hybrid in solutions containing 2 M NaCl, which causes partial but not quantitative dissociation into dimers (Feichtner et al., 1980). The intrinsic ^{3}ZnP decay rate constant is unaffected by the high salt, $k_D = 50$ s^{-1}, but the electron-transfer rate is cut to $k_t = 60$ s^{-1} by the increased dissociation. The decreased rate of electron transfer at high salt concentrations confirms that the (α_1,β_2) dimer is the primary electron-transfer unit, although we cannot rule out a small, but finite rate of transfer at longer distance in the (α_1,β_1) dimers. Studies of electron transfer under conditions of quantitative dimer formation will address this issue.

Discussion

The analytical results presented here demonstrate that the [Zn,Fe] mixed-metal Hb hybrids studied are pure, homogeneous proteins with 1:1 ZnP:FeP ratio. The spectrum of the reduced, [Zn,Fe^{II}], hybrid closely corresponds to that generated by summing equal contributions of ZnHb and Hb spectra. However, there are strong differences between the experimentally observed and computer-generated optical spectra for the oxidized, [Zn,Fe^{III}(H$_2$O)], hybrids, and the phenomenon appears to be associated with the Fe^{III} chains. Such differences, as well as those between the two hybrids, undoubtedly are related to the structural perturbations of the liganded ferriheme within the unliganded (T) quaternary structure

[5] We thank an anonymous referee for suggesting that this possibility be addressed explicitly.

[6] Recall that the oxidation reaction, Fe^{II}P + L $\rightarrow$ Fe^{III}(L)P + e$^-$, is formally and functionally identical with the ligation reaction, Fe^{II}P + L $\rightarrow$ Fe(L)P (Bull & Hoffman, 1975).

(Arnone et al., 1986). However, the $Fe^{III}(H_2O)P$ of the $[Zn^{II},Fe^{III}(H_2O)]$ hybrid appears to be uniquely sensitive to these effects. Further study of these anomalies may provide useful information on the nature of chain differences and subunit interactions in the hemoglobin tetramer.

The measurements reported here confirm the occurrence of $^3ZnP \rightarrow Fe^{III}P$ electron transfer within the (α_1,β_2) electron-transfer complex of the $[Fe^{III},Zn]$ hybrid hemoglobins. They demonstrate that (i) quenching of ^3ZnP by $Fe^{III}P$ is intramolecular and (ii) it occurs by electron transfer and not spin–quenching or energy transfer. One fundamental issue remains to be addressed: (iii) Does electron transfer proceed by a long-range, concerted process?

In general, amino acid residues are not easily reduced, and it is plausible a priori to assume that the electron-transfer process within the $[Zn,Fe^{III}]$ hybrids does not involve a stepwise, "hopping" transfer, in which an electron (or hole) resides for a finite interval on an intervening residue(s) as it proceeds from ^3ZnP to $Fe^{III}P$. However, even if such processes can occur, they *cannot* contribute to the electron-transfer rate constant, k_t, in Table I. This is because in general a process in which ^3ZnP reduces an arbitrary residue not only would contribute to the decay of the ^3ZnP if the electron proceeds on to reduce the ferriheme but also would contribute if the electron instead returned to the resulting ZnP^+ radical, as it must in the $[Zn,Fe^{II}]$ hybrid, whose hemes have been prereduced to the $Fe^{II}P$ state. Thus transient reduction of a protein residue, if present, should contribute to the base rate, k_D, whereas k_t measures *only* the long-range electron-transfer reaction.

This study also has shown that the rate of long-range electron transfer in the [Zn,Fe] hemoglobin hybrids can be changed by over an order of magnitude by changing the axial ligation of the $Fe^{III}P$. The sensitivity of an electron-transfer process to the properties of the acceptor (or donor) demonstrates that the rate-limiting step is indeed electron transfer and not a conformational interconversion (e.g., T → R switch) (Hoffman & Ratner, 1987).

The nature of the changes in the k_t with heme–ligand is not obvious. For example, ligand binding to the $Fe^{III}P$ will decrease its reduction potential, as has been demonstrated for the binding of F^- and N_3^- (Bull & Hoffman, 1975). The decreased exoergicity for the $^3ZnP \rightarrow Fe^{III}$–X transfer, as compared to $^3ZnP \rightarrow Fe^{III}H_2O$, would be expected to reduce k_t since, as we have suggested elsewhere (Peterson-Kennedy et al., 1986), the electron-transfer process is in the "normal" regime. Thus, the diminished k_t for X = F^- and CN^- is qualitatively as expected on energetic grounds, but the increase for X = Im is not.

Similarly, there is no simple correlation of k_t with the ferriheme spin state. In a high-spin ferriheme the iron ion is out of the plane, whereas in a low-spin ferriheme it is in-plane (Deatherage et al., 1976). The thermodynamic product of electron transfer is the high-spin, five-coordinate $Fe^{II}P$, in which the iron ion is out-of-plane. Thus, low-spin and high-spin ferriheme electron acceptors are expected to exhibit different reorganization energies and rates for reduction to the high-spin ferriheme state. However, X = Im and X = CN^- both form low-spin complexes and would be expected to exhibit roughly similar behavior, yet the former is reduced rapidly ($k_t \sim 200\ s^{-1}$) and the latter slowly ($k_t \sim 10\ s^{-1}$). Similarly, the k_t observed for the high-spin, X = F^- complex is much lower than that observed for the high-spin X = H_2O complex but identical with that observed for the low-spin X = CN^-, again contrary to expectations.

This discussion of spin state ignores some important details of heme chemistry, but further considerations do not appear to remove all anomalies. Specifically, X = CN^- is unlike the other ligands employed in that the *kinetic* product of electron transfer is expected to be the metastable low-spin, $Fe^{II}(CN)P$ (Keilin & Hartree, 1955) and not the high-spin, $Fe^{II}P$ thermodynamic product, and there is some indication that analogous intermediates might occur for the other X (Blumenfeld & Davidov, 1979). However, reduction of a low-spin $Fe^{III}P$ to give low-spin $Fe^{II}P$ should have a reduced reorganization energy and a correspondingly higher k_t, contrary to observation. We would not expect the additional decrease in exoergicity, probably less than 0.1–0.2 eV, that must accompany the formation of this metastable state to be more important than the major change in reorganization energy that must accompany formation of the thermodynamic product in other reactions. Indeed, the most obvious correlation among the k_t values for all the hybrid derivatives studied is with the net charge associated with the ferriheme acceptor: k_t is large when X is a neutral ligand and $Fe^{III}X$ is positively charged (X = H_2O and imid), and the electron-transfer process thus involves a charge shift; the rate is small when $Fe^{III}X$ is neutral (X = F^-, CN^-, N_3^-). Although quite possibly fortuitous, such a correlation has been anticipated (Pasman et al., 1985). Clearly, full characterization of a suite of [Zn,Fe-X] hybrids will be necessary to systematize these intriguing observations.

ACKNOWLEDGMENTS

We thank Drs. David Gingrich and Judy Nocek for assistance in preparing the manuscript.

Registry No. ZnP, 11075-07-3.

REFERENCES

Adler, A. D., Longo, F. R., Kampas, F., & Kim, J. (1970) *J. Inorg. Nucl. Chem. 32*, 2443.

Ampulski, R. S., Ayers, V. E., & Morell, S. A. (1969) *Anal. Biochem. 32*, 163–169.

Antonini, E., & Brunori, M. (1971) *Hemoglobin and Myoglobin in Their Reactions with Ligands*, North-Holland, Amsterdam.

Arnone, A., Rogers, P., Blough, N. V., McGourty, J. L., & Hoffman, B. M. (1986) *J. Mol. Biol. 188*, 693–706.

Bannerjee, R., & Cassoly, R. (1969) *J. Mol. Biol. 42*, 351.

Blough, N. V., Zemel, H., Hoffman, B. M., Lee, T. C. K., & Gibson, Q. H. (1980) *J. Am. Chem. Soc. 102*, 5683.

Blumenfeld, L. A., & Davidov, R. M. (1979) *Biochim. Biophys. Acta 549*, 255–280.

Brunori, M., Amiconi, G., Antonini, E., Wyman, J., & Winterhalter, L. H. (1970) *J. Mol. Biol. 49*, 461.

Bull, C., & Hoffman, B. M. (1975) *Proc. Natl. Acad. Sci. U.S.A. 72*, 3382–3386.

Bunn, H. F., & Forget, B. G. (1986) *Hemoglobin: Molecular, Genetic, and Clinical Aspects*, Saunders, Philadelphia.

Conrad, R. H., & Brand, L. (1978) *Biochemistry 17*, 777–787.

Crutchley, R. J., Ellis, W. R., Jr., & Gray, H. B. (1986) *Frontiers in Bioinorganic Chemistry*, 2nd ed. (Xavier, A. V., Ed.) pp 679–692, VCH, Weinheim, FRG.

Dale, R. E., Eisinger, J., & Blumberg, W. E. (1979) *Biophys. J. 26*, 161–194.

Deatherage, J. F., Loe, R. S., & Moffat, K. (1976) *J. Mol. Biol. 104*, 723–728.

DeVault, D. (1984) *Quantum Mechanical Tunnelling in Biological Systems*, 2nd ed., Cambridge University Press, Cambridge, U.K.

Douzou, P. (1974) *Methods Biochem. Anal. 22*, 401–512.
Eaton, W. A., & Hofrichter, J. (1981) *Methods Enzymol. 76*, 312–329.
Eaton, W. A., Hanson, L. K., Stephens, P. J., Sutherland, J. C., & Cunn, B. R. (1978) *J. Am. Chem. Soc. 100*, 4991–5003.
Feichtner, M. D., McLendon, G., & Bailey, M. W. (1980) *Biochem. Biophys. Res. Commun. 96*, 618–625.
Fermi, G., & Perutz, M. F. (1981) *Haemoglobin and Myoglobin: Atlas of Molecular Structures in Biology* (Phillips, D. C., & Richard, F. M., Eds.) Vol. 2, Oxford University Press, Oxford, U.K.
Geraci, G., Parkhurst, L. J., & Gibson, Q. H. (1969) *J. Inorg. Nucl. Chem. 32*, 2443.
Grassetti, D. R., & Murray, J. F. (1967) *Arch. Biochem. Biophys. 119*, 41–49.
Ho, P. S., Sutoris, C., Liang, N., Margoliash, E., & Hoffman, B. M. (1985) *J. Am. Chem. Soc. 107*, 1070–1071.
Hoffman, B. M. (1975) *J. Am. Chem. Soc. 97*, 1688–1694.
Hoffman, B. M., & Ratner, M. A. (1987) *J. Am. Chem. Soc.* (in press).
Isied, S. S., Worosila, G., & Atherton, S. J. (1982) *J. Am. Chem. Soc. 104*, 7659–7661.
Isied, S. S., Kuehn, C., & Worosila, G. (1984) *J. Am. Chem. Soc. 106*, 1722–1726.
Keilin, D., & Hartree, E. F. (1955) *Biol. J. 61*, 153–171.
Kirshner, A. G., & Tanford, C. (1964) *Biochemistry, 3*, 291–296.
Leonard, J. J., Yonetani, T., & Callis, J. B. (1974) *Biochemistry 13*, 1460–1464.
Liang, N., Kang, C. H., Ho, P. S., Margoliash, E., & Hoffman, B. M. (1986) *J. Am. Chem. Soc. 108*, 4665–4666.
Linder, L. E., Records, R., Barth, G., Bunnenberg, E., Djerassi, C., Hedlund, B. E., Rosenberg, A., Benson, E. S., Seamans, L., & Moscowitz, A. (1978) *Anal. Biochem. 90*, 474.
Marcus, R. A., & Sutin, N. (1985) *Biochim. Biophys. Acta 811*, 265–322.
Mawatari, K., Matsukawa, S., & Yoneyama, Y. (1983) *Biochim. Biophys. Acta 748*, 381.
Mayo, S. L., Ellis, W. R., Jr., Crutchley, R. J., & Gray, H. B. (1986) *Science (Washington, D.C.) 233*, 948–952.
McGourty, J. L., Blough, N. V., & Hoffman, B. M. (1983) *J. Am. Chem. Soc. 105*, 4470–4472.
McLendon, G., & Miller, J. R. (1985) *J. Am. Chem. Soc. 107*, 7811–7816.
McLendon, G. L., Winkler, J. R., Nocera, D. G., Mauk, M. R., Mauk, A. G., & Gray, H. B. (1985) *J. Am. Chem. Soc. 107*, 739–740.
McLendon, G., Miller, J. R., Simolo, K., Taylor, K., Mauk, A. G., & English, A. M. (1986) *ACS Symp. Ser. No. 307*, 150–165.
Pasman, P., Mes, G. F., Koper, N. W., & Verhoeven, J. W. (1985) *J. Am. Chem. Soc. 107*, 5839–5843.
Perutz, M. F. (1979) *Annu. Rev. Biochem. 48*, 327–386.
Peterson-Kennedy, S. E., McGourty, J. L., & Hoffman, B. M. (1984) *J. Am. Chem. Soc. 106*, 5010–5012.
Peterson-Kennedy, S. E., McGourty, J. L., Ho, P. S., Sutoris, C. J., Liang, N., Zemel, H., Blough, N. V., Margoliash, E., & Hoffman, B. M. (1985) *Coord. Chem. Rev. 64*, 125–133.
Peterson-Kennedy, S. E., McGourty, J. L., Kalweit, J. A., & Hoffman, B. M. (1986) *J. Am. Chem. Soc. 108*, 1739–1746.
Poulos, T. L., & Kraut, J. (1980) *J. Biol. Chem. 155*, 10322–10330.
Poulos, T. L., & Finzel, B. C. (1984) *Pept. Protein Rev. 4*, 115.
Riggs, A. (1981) *Methods Enzymol. 76*, 5.
Rose, E. J., & Hoffman, B. M. (1983) *J. Am. Chem. Soc. 105*, 286–2873.
Scholler, D. M., Wang, M.-Y. R., & Hoffman, B. M. (1978) *Methods Enzymol. 3C*, 487–493.
Scott, R. A., Mauk, A. G., & Gray, H. B. (1985) *J. Chem. Educ. 62*, 932–938.
Simolo, K. P., McLendon, G. L., Mauk, M. R., & Mauk, A. G. (1984) *J. Am. Chem. Soc. 106*, 5012–5013.
Stanford, M. A., Swartz, J. C., Phillips, T. E., & Hoffman, B. M. (1980) *J. Am. Chem. Soc. 102*, 4492–4499.
Tollin, G., Meyer, T. E., & Cusanovich, M. A. (1986) *Biochim. Biophys. Acta 253*, 29–41.
Turro, N. J. (1978) *Modern Molecular Photochemistry*, 2nd ed., Benjamin/Cummings, Menlo Park, CA.
Winkler, J. R., Nocera, D. G., Yocom, K. M., Bordignon, E., & Gray, H. B. (1982) *J. Am. Chem. Soc. 104*, 5798–5800.
Yip, Y. K., Waks, M., & Beychok, S. (1977) *Proc. Natl. Acad. Sci. U.S.A. 74*, 64.
Zemel, H., & Hoffman, B. M. (1981) *J. Am. Chem. Soc. 103*, 1192–1201.